

Construction of polyaniline/molybdenum sulfide nanocomposite: characterization and its electrocatalytic performance on nitrite

Ya Zhang^{1,2} · Peng Chen¹ · Fangfang Wen¹ · Chen Huang¹ · Honggui Wang¹

Received: 31 October 2015 / Revised: 7 December 2015 / Accepted: 29 December 2015 / Published online: 25 January 2016
© Springer-Verlag Berlin Heidelberg 2016

Abstract A polyaniline/molybdenum sulfide (PANI-MoS₂) nanocomposite was synthesized via a hydrothermal method and in situ polymerization, respectively. Fourier transform infrared spectroscopy (FT-IR) and X-ray diffraction (XRD) results indicated that the PANI and MoS₂ had been successfully composited. Cyclic voltammetry (CV) result showed that the PANI-0.1 g MoS₂-modified glassy carbon electrode (GCE) exhibited excellent electrochemical activity in a 0.1 M phosphate-buffered saline (PBS) solution compared to the MoS₂, PANI, and other PANI-MoS₂ composite-modified GCEs. CV result also confirmed that nitrite could be oxidized by the PANI-0.1 g MoS₂ in a pH 5.0 PBS solution. The amperometric response result indicated that the PANI-0.1 g MoS₂-modified GCE could be used to determine a nitrite concentration in a wide linear range of 4.0 and 4834 μM with a detection limit of 1.5 μM. The anti-interference property and real sample analysis was also proposed.

Keywords Polyaniline · MoS₂ · Electrocatalysis · Nitrite · Sensor

Introduction

Nitrites are used in a large amount as a food additive, corrosion inhibitor, and fertilizing agent. It is recognized as an alarming pollutant to the environment and human health [1]. The excessive ingestion of nitrites via the dietary intake has potential toxic and carcinogenic effects [2]. The maximum permitted level of nitrite established by the European Drinking Water Directive is 0.02 mg L⁻¹ [3]. Therefore, its determination is of great urgent for both environmental and public health reasons. The electrochemical approach is rapid, highly selective, and sensitive. Furthermore, it is considered to be an environmentally friendly method because no additional chemical loading is required. There are different electrochemical methods, which are employed to construct sensors, including amperometry, voltammetry, potentiometry, coulometry, and electrochemical impedance spectroscopy (EIS) [4]. Amperometry is widely applied in chemical and biological sciences especially in the field of sensor and biosensor researches [5, 6].

Usually, the electrochemical behavior of nitrite is poor at the conventional solid electrode surfaces. A good way of solving this problem is using modified electrodes. Various materials have been used for fabricating electrode surfaces, including conducting polymer [3, 7]; carbon materials [8–10]; and noble metals [1, 2, 11]. Among them, polyaniline (PANI) is considered as a promising substrate for determination of nitrite [3] for its excellent electronic property. Although the electrochemical determination of nitrite has got the successful development, an electrochemical sensor with better properties, such as easy manufacture, low price, wider operational potential window, renewable surface, and environmentally friendly, is still a challenge.

Molybdenum sulfide (MoS₂), with a two-dimensional layered structure, has been successfully established as a new

✉ Honggui Wang
wanghg@yzu.edu.cn

¹ Jiangsu Key Laboratory of Environmental Material and Engineering, School of Environmental Science and Engineering, Yangzhou University, Yangzhou 225127, People's Republic of China

² School of Chemistry and Chemical Engineering, Yangzhou University, Yangzhou 225009, People's Republic of China

paradigm in the chemistry of nanomaterials in recent years due to its excellent electronic and optical properties [12–14]. Besides, MoS₂ nanosheets can be facilely synthesized in large scale and directly dispersed in aqueous solution without the need of surfactants or oxidation treatment [13]. Recently, Huang et al. reported a novel two-dimensional graphene analog molybdenum disulfide/multiwalled carbon nanotube/Au nanoparticle enzyme system with excellent electrochemical properties and ultrasensitive DNA detection ability [13]. Another MoS₂-based composite fabricated by Huang and co-workers can be used as a bisphenol A sensor [15]. Most recently, PANI was found to effectively improve the conductivity and stability of MoS₂ and has been utilized in designing MoS₂/PANI composites with enhanced electrochemical performances [16–18]. However, to the best of our knowledge, no PANI/MoS₂ composite-modified glassy carbon electrodes (GCEs) have yet been reported for nitrite determination.

In this work, a PANI-MoS₂ composite was synthesized via in situ polymerization of an aniline monomer in the presence of MoS₂. The PANI-MoS₂-modified GCE showed excellent electrochemical activity in an acid solution and enhanced electrocatalytic performance on nitrite oxidation. The factors affecting nitrite determination and the possible mechanism of the electrocatalytic process were also presented.

Experimental section

Synthesis of PANI-MoS₂ composite

MoS₂ was prepared via a hydrothermal method as reported previously [19]. A mixture of 0.5 g of Na₂MoO₄ and 0.8 g of

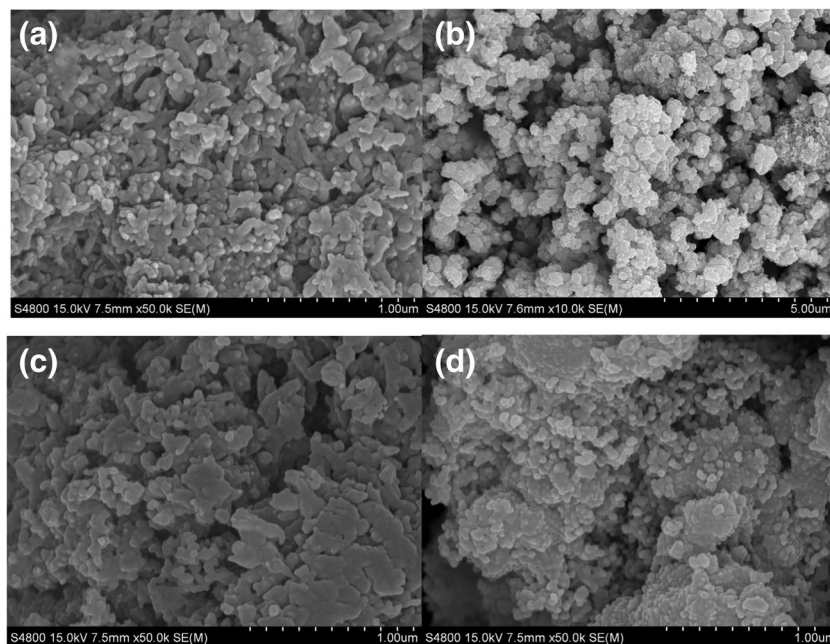
L-cysteine was dissolved in 80 mL deionized (DI) water and then transferred into a 100-mL Teflon-lined stainless steel autoclave and heated at 180 °C for 20 h. After cooling naturally, the black precipitates were collected by centrifugation, washed with DI water and ethanol, and dried in a vacuum oven at 70 °C overnight.

The typical preparation procedures of the PANI-MoS₂ nanocomposites are as follows: 1.17 mL aniline monomer and 3.87 mL HCl were dissolved in 125 mL DI water. Then, 3.87 mL HCl, a certain amount of MoS₂, and 2.85 g (NH₄)₂S₂O₈ dissolved in 125 mL of DI water were dropped into the above solution with stirring at room temperature. After having been stirred for about 10 h, the resulting products were separated by centrifugation and finally washed with deionized water until the precipitate was colorless. The resulting products were dried under dynamic vacuum at 65 °C for 24 h. The PANI-MoS₂ composites containing 0.1 and 0.5 g MoS₂ were denoted as PANI-0.1 g MoS₂ and PANI-0.5 g MoS₂, respectively. As a control experiment, PANI was prepared under the same conditions without adding MoS₂.

Preparation of PANI, MoS₂, and PANI-MoS₂ composite-modified electrode

Prior to modification, a glassy carbon electrode (GCE) was polished with an alumina slurry of 0.5 μM on polishing cloth with water and then thoroughly rinsed with water and sonicated in a DI water bath for 10 min before use. For preparation of PANI, MoS₂, and PANI-MoS₂-modified electrodes, 4 mg samples were dispersed in 0.8 mL DI water and 0.2 mL ethanol by ultrasonication for 30 min to obtain a homogeneous suspension (4.0 mg mL⁻¹). Then, a certain amount of the

Fig. 1 SEM images of **a** PANI, **b** MoS₂, **c** PANI-0.1 g MoS₂, and **d** PANI-0.5 g MoS₂



suspension was dropped onto the surface of GCE and dried at room temperature.

Electrochemical properties

All electrochemical experiments were performed in the electrolytic cell consisted of a glassy carbon (GC) or a modified GC working electrode (3 mm diameter, CHI), a platinum wire counter electrode, and a saturated calomel electrode (SCE) as reference on a model CHI 660 E electrochemical workstation. All potentials were referred to as a SCE.

Characterization

The Fourier transform infrared spectroscopy (FT-IR) spectra of the samples were measured on a Cary 610/670 microscope (Varian, USA). Scanning electron microscopy (SEM) was examined on a field emission scanning electron microanalyzer (Hitachi S-4800, Japan). The X-ray diffraction (XRD) patterns were obtained by a Bruker D8 advance X-ray diffractometer using monochromatic Cu K α radiation ($\lambda = 1.5406 \text{ \AA}$) with an accelerating voltage of 40 kV and a current of 40 mA. The pH values of the solutions were determined with a PHS-3C pH meter.

Results and discussion

Characterization of PANI, MoS₂, and PANI-MoS₂ composite

The morphology of the as-obtained samples was examined by SEM. PANI (Fig. 1a) is constructed of random short nanorod with diameters of 80–100 nm and lengths varying from 100 to 200 nm. As can be seen in the SEM image (Fig. 1b), the MoS₂ is flowerlike with the overlapped or coalesced sheet-like subunits structure. Figure 1c, d displays the SEM images of PANI-0.1 g MoS₂ and PANI-0.5 g MoS₂, respectively, which indicate that the image of the composite is highly dependent on the ratio of PANI and MoS₂. The image of PANI-0.1 g MoS₂ is similar to that of the pure PANI, while PANI-0.5 g MoS₂ tends to aggregate. This result gives us a hint that the electrochemical activity of PANI-0.1 g MoS₂ may be better than that of PANI-0.5 g MoS₂ for the aggregation.

The FT-IR spectra of PANI, MoS₂, and PANI-MoS₂ composite are shown in Fig. 2a. The peaks observed at about 806 and 1120 cm⁻¹ at the curves of PANI and PANI-MoS₂ composite are attributed to the C–H out-of-plane and in-plane bending in Q and B rings, respectively [20, 21]. The peak appeared at about 1305 cm⁻¹ at the curve of PANI-MoS₂ composite is associated with C–N stretching of an aromatic

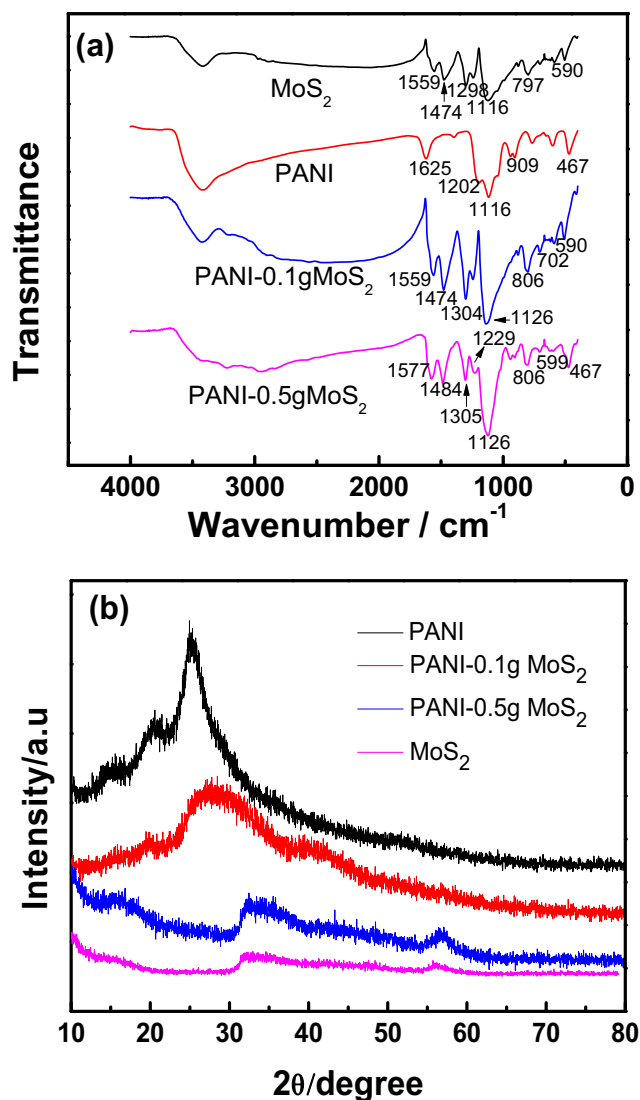


Fig. 2 a Infrared spectra and b XRD of PANI, MoS₂, PANI-0.1 g MoS₂, and PANI-0.5 g MoS₂

amine [21, 22]. The peak located at about 591 cm⁻¹ on the curve of PANI is attributed to C–C bonding mode of aromatic ring [23], while the weak peaks at about 590 cm⁻¹ at the curves of MoS₂ and the MoS₂-based composite correspond to γ_{as} Mo–S vibration [24].

Figure 2b shows the XRD patterns of the as-obtained samples. Broad diffraction peaks between 10° and 30° can be observed in the XRD patterns of PANI, which are due to the parallel and perpendicular periodicity of the polymer (PANI) chain [25]. The peak diffracted at $2\theta = 20.2$ and 25.2 in the XRD pattern which shows low crystallinity of the conductive polymers due to the repetition of benzenoid and quinoid rings in PANI chains [25]. As for the pure MoS₂, the detected XRD pattern peaks at $2\theta = 32.1^\circ$, 47.1° , 48.9° , and 56.6° can be assigned to the orthorhombic phase of MoS₂ (JCPDS no. 37-1492), respectively [14]. In the case of the PANI-0.1 g MoS₂ composite, the presence of diffraction peaks at

$2\theta = 20.1^\circ$, 27.6° , and 56.8° indicates that PANI grew on MoS_2 . According to the results of SEM, FT-IR, and XRD, PANI and MoS_2 have been successfully composited.

Electrochemical activity and stability of PANI- MoS_2 composite-modified GCE

To evaluate the catalytic ability of the PANI- MoS_2 nanocomposite-modified GCE, cyclic voltammetry (CV) experiments were performed in a pH 5.0, 0.1 M phosphate-buffered saline (PBS) solution. Figure 3a displays the CVs of the PANI, MoS_2 , and PANI- MoS_2 -modified GCE in a pH 5.0, 0.1 M PBS solution, at a scan rate of 50 mV s^{-1} . As shown in Fig. 3a, the CV curves of the PANI-0.1 g MoS_2 nanocomposite-modified GCEs have the largest area than those of PANI and MoS_2 , which indicates that the deposition of PANI-0.1 g MoS_2 nanocomposite improves the electrochemical activity of the

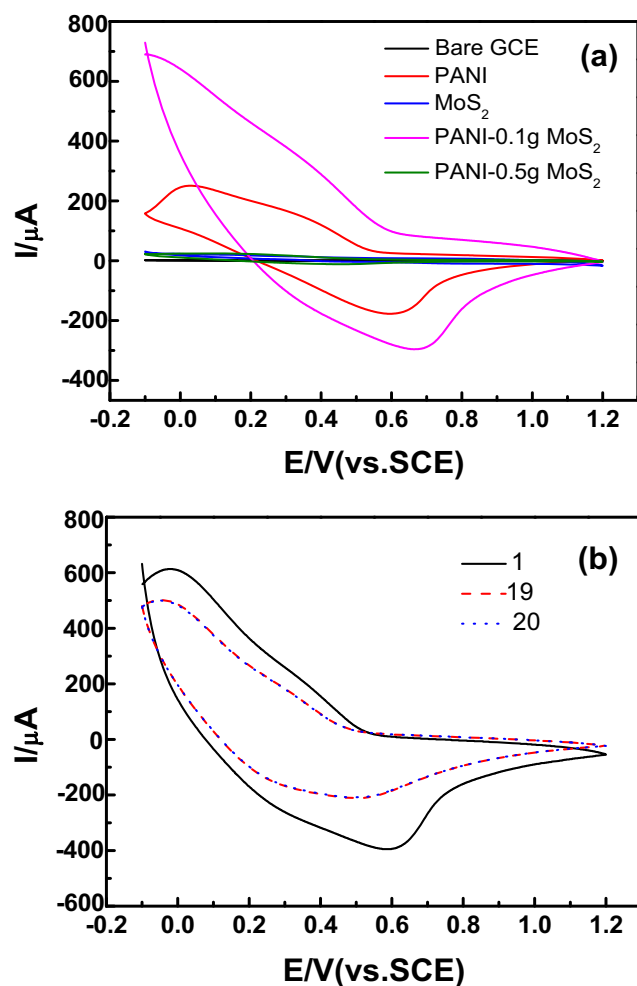


Fig. 3 a CVs of bare GCE, PANI, MoS_2 , PANI-0.1 g MoS_2 , and PANI-0.5 g MoS_2 -modified GCE in a pH 5.0, 0.1 M PBS solution at a scan rate of 50 mV s^{-1} . b CVs of PANI-0.1 g MoS_2 in a pH 5.0, 0.1 M PBS solution; the curves indicate the 1st cycle (black solid), the 19th cycle (red dash), and the 20th cycle (blue dot), at a scan rate of 20 mV s^{-1}

electrode. However, when the ratio of MoS_2 increases in the PANI- MoS_2 nanocomposite, the electrochemical activity of the PANI-0.5 g MoS_2 -modified GCEs decreases. As mentioned above, the SEM image of PANI-0.5 g MoS_2 is more aggregated than PANI and PANI-0.1 g MoS_2 . The excellent electrochemical property of the PANI-0.1 g MoS_2 composite is attributed to the integral composite structure and the synergistic effect between PANI and MoS_2 substrates. Figure 3b depicts the 1st, 19th, and 20th cycle of the CV of the PANI- MoS_2 -modified GCE immersed in a pH 5.0, 0.1 M PBS solution. It can be clearly seen in Fig. 3b that the electrochemical activity of PANI- MoS_2 decreases obviously at first; however, it reaches the stable state after 19–20 cycles.

Electrocatalytic oxidation of nitrite at PANI- MoS_2 nanocomposite-modified GCE

To evaluate the nitrite catalytic ability of the PANI-0.1 g MoS_2 nanocomposite, CV experiments were performed in a pH 5.0, 0.1 M PBS solution with and without various concentrations of nitrite. As can be seen in Fig. 4, the current of the oxidation peaks (1.05 V) increases when increasing the concentration of nitrite, which indicates that nitrite could be oxidized by the PANI-0.1 g MoS_2 [26]. The corresponding transformation is shown as follows:



Factors influencing the oxidation of nitrite

Figure 5 shows the CVs of the PANI-0.1 g MoS_2 -modified GCE in a pH 5.0, 0.1 M PBS solution at various amounts

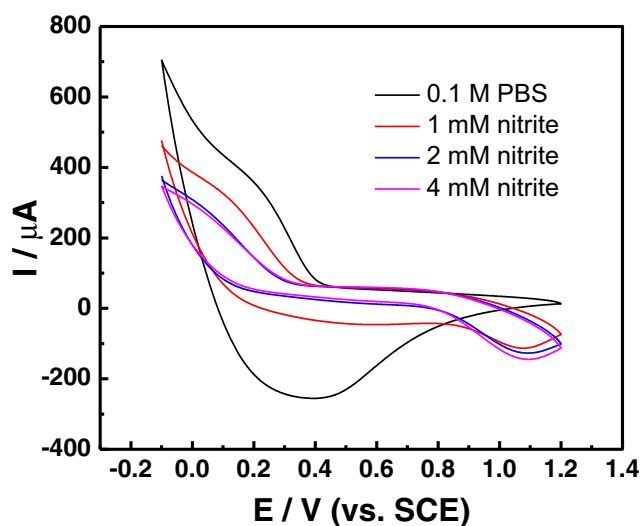


Fig. 4 CVs of the PANI-0.1 g MoS_2 nanocomposite-modified GCE in a pH 5.0, 0.1 M PBS solution containing various concentrations of nitrite, at a scan rate of 50 mV s^{-1}

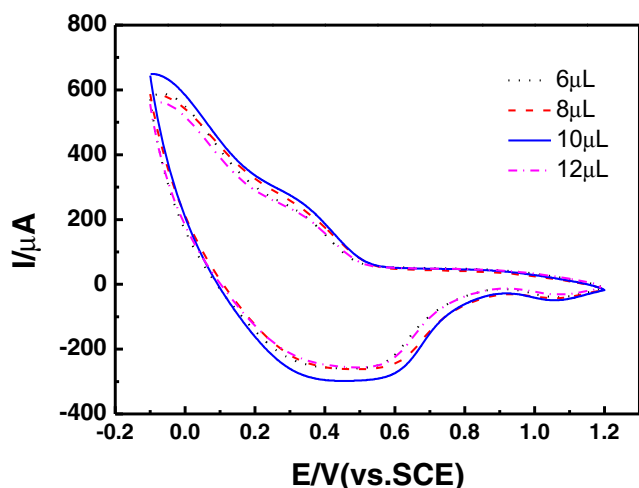


Fig. 5 CVs of different contents of the PANI-0.1 g MoS₂ nanocomposite-modified GCE in a pH 5.0, 0.1 M PBS solution with 1 mM nitrite, at a scan rate of 50 mV s⁻¹

of PANI-0.1 g MoS₂ deposition (6.0–12.0 μL). The oxidation peak current increases as the deposition amount increases from 6.0 to 10.0 μL, while the peak current stops increasing when the deposition amount increases to 12.0 μL. This is because a higher amount of sample deposition may initiate the aggregation of PANI-0.1 g MoS₂ and thereby inhibit the catalytic activity of PANI-0.1 g MoS₂.

Figure 6a shows the CVs of the PANI-0.1 g MoS₂-modified GCE in a 0.1 M PBS solution with 1 mM nitrite (pH 5.0) at different scan rates (10 to 100 mV s⁻¹). As shown in Fig. 6a, the current of the oxidation peak at about 1.05 V increases with increasing the scan rate. The relationship between the oxidation peak current (*I_p*) and the scan rate is shown in Fig. 6b, in which a straight line is obtained ($Y=4.209-2.252X$, $R^2=0.988$). The anodic oxidation peak increases linearly with scan rates, indicating a diffusion-controlled electrocatalytic process.

The effect of solution pH on the electrochemical response of 1 mM nitrite was investigated in the pH range of 3.0 to 7.0 in a 0.1 M PBS solution. It can be clearly seen in Fig. 7 that the current densities increase when increasing the pH from 3.0 and 5.0. When the solution pH is higher than 5.0, the current densities of the CV curves decrease due to the shortage of proton and the decrease of electrochemical activity of PANI [2]. The maximal current density is obtained at pH 5.0; therefore, the pH 5.0 is selected as the optimum pH value in our experiments.

Amperometric determination of nitrite

Figure 8a, b displays the typical amperometric response of the PANI-0.1 g MoS₂ upon successive addition of 1.0×10^{-4} , 5.0×10^{-4} , 1.0×10^{-3} , 5.0×10^{-3} , and 1.0×10^{-2} M of nitrite in a 0.1 M PBS solution (pH 5.0) at an applied potential of

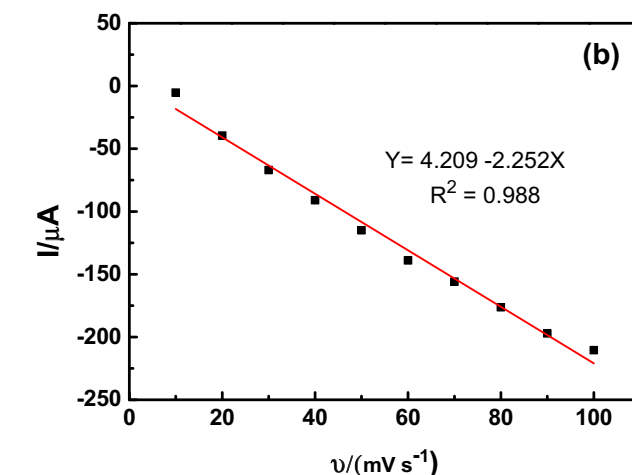
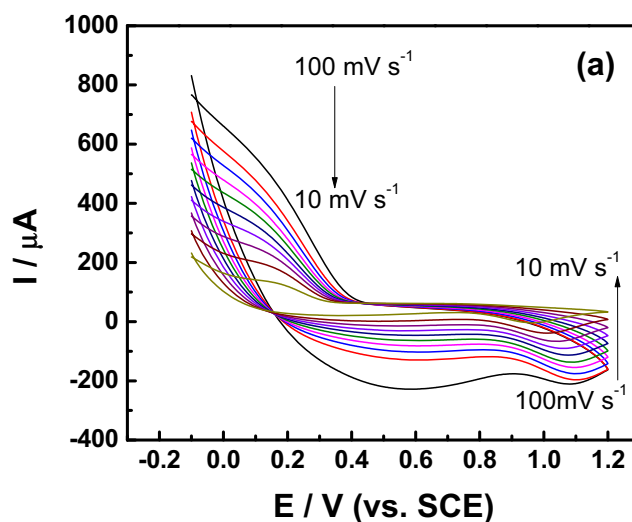


Fig. 6 a CVs of the PANI-0.1 g MoS₂ nanocomposite-modified GCE in a 0.1 M PBS solution with 1 mM nitrite (pH 5.0) at different scan rates (10–100 mV s⁻¹). b The relationship between the reduction peak current (*I_p*) and the scan rate

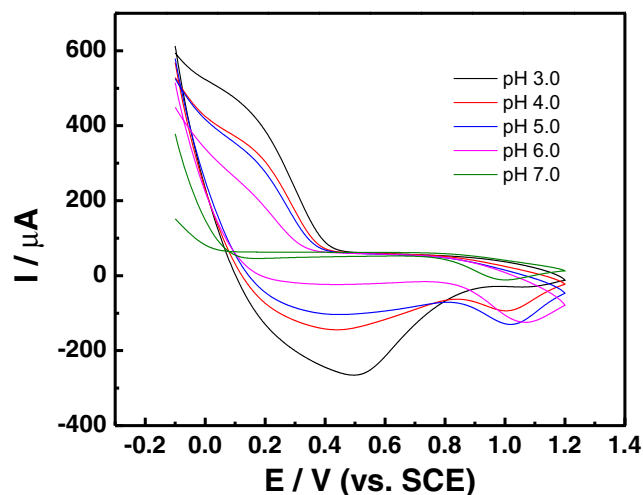


Fig. 7 CVs of the PANI-0.1 g MoS₂ nanocomposite-modified GCE in a 0.1 M PBS solution with 1 mM nitrite at different solution pH values (pH 3–7), at a scan rate of 50 mV s⁻¹

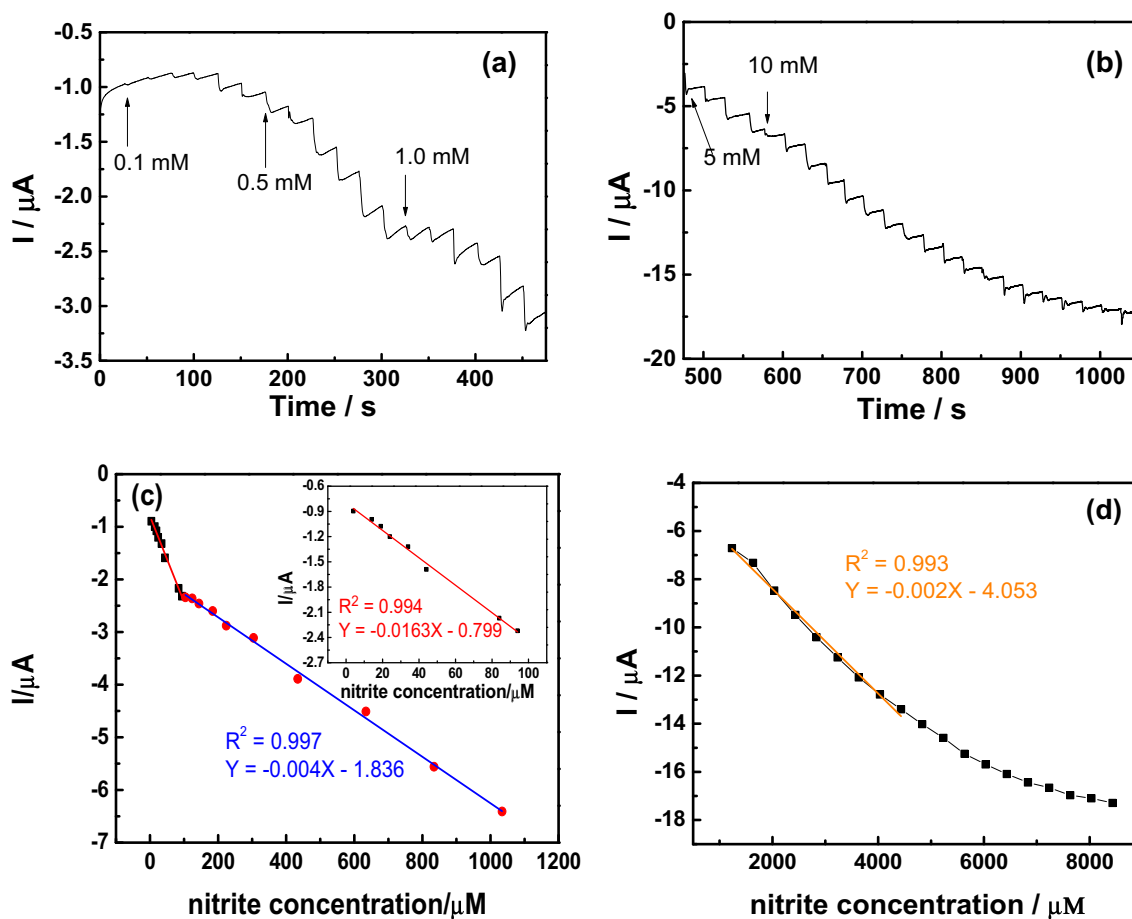


Fig. 8 **a, b** Amperometric response curves of the PANI-0.1 g MoS₂-modified GCE in a pH 5.0, 0.1 M PBS solution. **c, d** Plot of response currents vs. nitrite concentrations. PANI-0.1 g MoS₂ deposition = 10 μ L

0.9 V. Figure 8c, d shows the relationship between the response current of the PANI-0.1 g MoS₂ and the concentration of nitrite. As shown in Fig. 8c, d, the response currents at the PANI-0.1 g MoS₂/GCE are proportional to the concentration of nitrite in the ranges of 4.0–94 μ M ($R^2=0.994$), 94–1034 μ M ($R^2=0.997$), and 1034–4834 μ M ($R^2=0.993$). The corresponding sensitivities of the PANI-0.1 g MoS₂/GCE are 0.68, 6.50, and 28.68 mA μ M⁻¹ cm⁻², respectively. Based on the confidence limits of the regression equation and for a factor of 3, the limit of detection is 1.5 μ M, which is lower

enough than the drinking water limit quantity postulated by the WHO (43 μ M) [27]. It should be noted that the performance of the PANI-0.1 g MoS₂/GCE (linear range and detection limit) is quite comparable with other nitrite sensors based on noble metals or polymers (Table 1) [28–34].

Interference study and real sample analysis

The response of the PANI-0.1 g MoS₂ sensors to some common coexisting ions with nitrite in real samples was

Table 1 Comparison of PANI-MoS₂ with other matrices for nitrite sensors

Electrode material	Linear range (μ M)	Detection limit (μ M)	Reference
PtAu/Ch/GCE	0.2–600	0.06	[28]
CR-GO/GCE	8.9–167	1.0	[29]
TOAB/ZnP-C60/GCE	2.0–164	1.44	[30]
AgPs-ILCPE	50–1000	3	[31]
Fe ₃ O ₄ /r-GO/GCE	1–210	0.3	[32]
Poly(PyY)/PGE	1–100	0.5	[33]
Hb/PLE	10–220	5.0	[34]
PANI-MoS ₂ /GCE	4.0–4834	1	This work

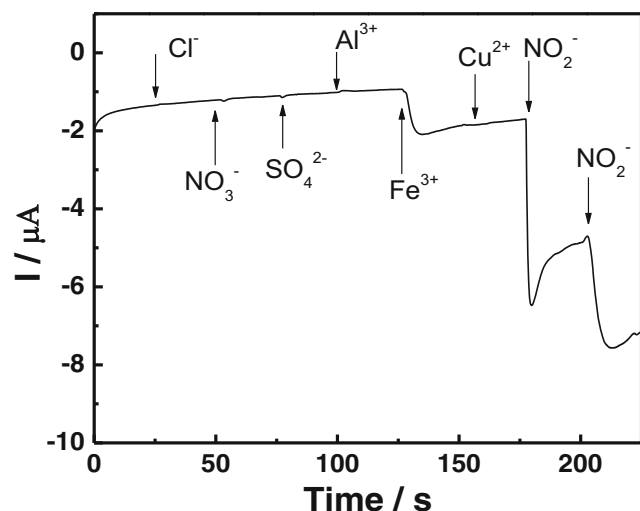
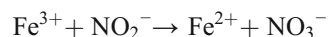


Fig. 9 Response of the PANI-0.1 g MoS₂ sensor to successive additions of various compounds at concentrations of 1.0×10^{-3} M. Electrolyte = 0.1 M PBS, pH 5.0. Polarization potential = 0.9 V

investigated by the addition of various ions to a 0.1 M PBS solution in the presence of 0.5 mM nitrite. Figure 9 shows the experimental results of the interference study. The successive addition of 1 mM Cl⁻, NO₃⁻, SO₄²⁻, Cu²⁺, and Al³⁺ has no interference on the determination of nitrite, while Fe³⁺ exhibits obvious interference. This is probably attributed to the reaction of Fe³⁺ and nitrite.



Amperometric measurement was used to test the practical applicability of proposed sensor for the determination of nitrite from real samples. Table 2 shows the experimental verification of the method on real samples. Excellent recovery values are achieved for both drinking water and river water samples.

Conclusions

In this work, a PANI-MoS₂ nanocomposite-modified GCE was fabricated. The CV result showed that the PANI-0.1 g

MoS₂/GCE exhibits excellent electrochemical activity and electrocatalytic performance on nitrite in a pH 5.0 PBS solution. The amperometric response results indicated that the response currents at the PANI-0.1 g MoS₂/GCE were proportional to the concentration of nitrite in the range of 4.0–94 μM ($R^2=0.994$), 94–1034 μM ($R^2=0.997$), and 1034–4834 μM ($R^2=0.993$). The corresponding sensitivities of the PANI-0.1 g MoS₂/GCE were 0.68, 6.50, and 28.68 mA μM⁻¹ cm⁻², respectively.

Acknowledgments This work was supported by the National Natural Science Foundation of China (No. 21307104), Natural Science Foundation of Jiangsu Province, China (No. BK20130438, BK 20150451), Jiangsu Key Laboratory of Environmental Material and Engineering (K13059, K14015), and the Priority Academic Program Development of Jiangsu Higher Education Institutions. We thank the Testing Center of Yangzhou University for sample characterization.

References

- Zhang Y, Zhao YH, Yuan S, Wang HG, He CD (2013) Electrocatalysis and detection of nitrite on a reduced graphene/Pd nanocomposite modified glassy carbon electrode. *Sens Actuators B Chem* 185:602–607
- Li SS, Hu YY, Wang AJ, Weng XX, Chen JR, Feng JJ (2015) Simple synthesis of worm-like Au–Pd nanostructures supported on reduced graphene oxide for highly sensitive detection of nitrite. *Sens Actuators B Chem* 208:468–474
- Zhang Y, Yin J, Wang K, Chen P, Ji L (2013) Electrocatalysis and detection of nitrite on a polyaniline-Cu nanocomposite modified glassy carbon electrode. *J Appl Polym Sci* 128:2971–2976
- Voitechovič E, Bratov A, Abramova N, Razumienė J, Kirsanov D, Legin A, Lakshmi D, Piletsky S, Whitcombe M, Ivanova-Mitseva PK (2015) Development of label-free impedimetric platform based on new conductive polyaniline polymer and three-dimensional interdigitated electrode array for biosensor applications. *Electrochim Acta* 173:59–66
- Cardoso WS, Gushikem Y (2005) Electrocatalytic oxidation of nitrite on a carbon paste electrode modified with Co(II) porphyrin adsorbed on SiO₂/SnO₂/phosphate prepared by the sol–gel method. *J Electroanal Chem* 583:300–306
- Kamyabi MA, Aghajanloo F (2008) Electrocatalytic oxidation and determination of nitrite on carbon paste electrode modified with oxovanadium(IV)-4-methyl salophen. *J Electroanal Chem* 614: 157–165
- Rajalakshmi K, John SA (2015) Highly sensitive determination of nitrite using FMWCNTs-conducting polymer composite modified electrode. *Sens Actuators B Chem* 215:119–124
- Innocenzo GC, Michela C (2014) Highly dispersed rhodium particles on multi-walled carbon nanotubes for the electrochemical reduction of nitrate and nitrite ions in acid medium. *Electrochim Acta* 138:447–453
- Ye FY, Feng CQ, Jiang JB, Han S (2015) Simultaneous determination of dopamine, uric acid and nitrite using carboxylated graphene oxide/lanthanum modified electrode. *Electrochim Acta* 182:935–945
- Zhou L, Wang JP, Gai L, Li DJ, Li YB (2013) An amperometric sensor based on ionic liquid and carbon nanotube modified composite electrode for the determination of nitrite in milk. *Sens Actuators B Chem* 181:65–70

Table 2 Experimental verification of the method on real samples

Sample	Theoretical [nitrite]/μM	Practical [nitrite]/μM	Recovery (%)	RSD ($n=5$, %)
Drinking water	6.00	5.79	96.50	1.99
	30.00	30.16	100.53	0.93
	300.00	297.30	99.10	1.27
River water	6.00	6.24	100.40	0.92
	30.00	29.59	98.63	1.66
	300.00	302.77	100.92	1.53

RSD relative standard deviation

11. Liu Y, Zhou J, Gong J, Wu WP, Bao N, Pan ZQ, Gu HY (2013) The investigation of electrochemical properties for $\text{Fe}_3\text{O}_4@\text{Pt}$ nanocomposites and an enhancement sensing for nitrite. *Electrochim Acta* 111:876–887
12. Huang KJ, Wang L, Li J, Liu YM (2013) Electrochemical sensing based on layered MoS_2 -graphene composites. *Sens Actuators B Chem* 178:671–677
13. Huang KJ, Liu YJ, Wang HB, Wang YY, Liu YM (2014) Sub-femtomolar DNA detection based on layered molybdenum disulfide/multi-walled carbon nanotube composites, Au nanoparticle and enzyme multiple signal amplification. *Biosens Bioelectron* 55:195–202
14. Fang LX, Huang KJ, Liu Y (2015) Novel electrochemical dual-aptamer-based sandwich biosensor using molybdenum disulfide/carbon aerogel composites and Au nanoparticles for signal amplification. *Biosens Bioelectron* 71:171–178
15. Huang KJ, Liu YJ, Liu YM, Wang LL (2014) Molybdenum disulfide nanoflower-chitosan-Au nanoparticles composites based electrochemical sensing platform for bisphenol A determination. *J Hazard Mater* 276:207–215
16. Zhang CF, Wang ZY, Guo ZP, Lou XW (2012) Synthesis of MoS_2 -C one-dimensional nanostructures with improved lithium storage properties. *ACS Appl Mater Interfaces* 4:3765–3768
17. Yang LC, Wang SN, Mao JJ, Deng JW, Gao QS, Tang Y, Schmidt OG (2013) Hierarchical MoS_2 /polyaniline nanowires with excellent electrochemical performance for lithium-ion batteries. *Adv Mater* 25:1180–1184
18. Hu LR, Ren YM, Yang HX, Xu Q (2014) Fabrication of 3D hierarchical MoS_2 /polyaniline and MoS_2 /C architectures for lithium-ion battery applications. *ACS Appl Mater Interfaces* 6:14644–14652
19. Sen UK, Mitra S (2013) High-rate and high-energy-density lithium-ion battery anode containing 2D MoS_2 nanowall and cellulose binder. *ACS Appl Mater Interfaces* 5:1240–1247
20. Chen SG, Wei ZD, Qi XQ, Dong LC, Guo YG, Wan LJ, Shao ZG, Li L (2012) Nanostructured polyaniline-decorated $\text{Pt/C}@\text{PANI}$ core-shell catalyst with enhanced durability and activity. *J Am Chem Soc* 134:13252–13255
21. Zhang K, Zhang LL, Zhao XS, Wu J (2010) Graphene/polyaniline nanofiber composites as supercapacitor electrodes. *Chem Mater* 22:1392–1401
22. Liu H, Zhang F, Li WY, Zhang XL, Lee CS, Wang WL, Tang YB (2015) Porous tremella-like MoS_2 /polyaniline hybrid composite with enhanced performance for lithium-ion battery anodes. *Electrochim Acta* 167:132–138
23. Mostafaei A, Zolriasatein A (2012) Synthesis and characterization of conducting polyaniline nanocomposites containing ZnO nanorods. *Prog Nat Sci Mater* 22(4):273–280
24. Liu SS, Zhang XB, Shao H, Xu J, Chen FY, Feng Y (2012) Preparation of MoS_2 nanofibers by electrospinning. *Mater Lett* 73:223–225
25. Shi L, Wang X, Lu L, Yang X, Wu X (2009) Preparation of TiO_2 /polyaniline nanocomposite from a lyotropic liquid crystalline solution. *Synth Met* 159:2525–2529
26. Zhou Y, Xian HY, Li F, Wu SN, Lu QF, Li YX, Wang L (2010) Construction of hybrid nanocomposites containing Pt nanoparticles and poly(3-methylthiophene) nanorods at a glassy carbon electrode: characterization, electrochemistry, and electrocatalysis. *Electrochim Acta* 55:5905–5910
27. World Health Organization (2011) Guidelines for drinking-water quality, 4th edn. WHO, Geneva
28. Wang P, Zhou FY, Wang ZW, Lai C, Han XG (2015) Substrate-induced assembly of PtAu alloy nanostructures at choline functionalized monolayer interface for nitrite sensing. *J Electroanal Chem* 750:36–42
29. Mani V, Periasamy AP, Chen SM (2012) Highly selective amperometric nitrite sensor based on chemically reduced graphene oxide modified electrode. *Electrochem Commun* 17:75–78
30. Wu H, Fan S, Jin X, Zhang H, Chen H, Dai Z, Zou X (2014) Construction of a zinc porphyrin-fullerene-derivative based nonenzymatic electrochemical sensor for sensitive sensing of hydrogen peroxide and nitrite. *Anal Chem* 86:6285–6290
31. Menart E, Jovanovski V, Hočevar SB (2015) Silver particle-decorated carbon paste electrode based on ionic liquid for improved determination of nitrite. *Electrochem Commun* 52:45–48
32. Teymourian H, Salimi A, Khezrian S (2013) Fe_3O_4 magnetic nanoparticles/reduced graphene oxide nanosheets as a novel electrochemical and bioelectrochemical sensing platform. *Biosens Bioelectron* 49:1–8
33. Dağcı K, Alanyahoğlu M (2013) Electrochemical preparation of polymeric films of pyronin Y and its electrocatalytic properties for amperometric detection of nitrite. *J Electroanal Chem* 711:17–24
34. Majidi MR, Saadatirad A, Alipour E (2013) Pencil lead electrode modified with hemoglobin film as a novel biosensor for nitrite determination. *Electroanalysis* 25:1742–1750